



HAL
open science

Design optimization of an axial-field eddy-current magnetic coupling based on magneto-thermal analytical model

Julien Fontchastagner, Thierry Lubin, Smail Mezani, Noureddine Takorabet

► To cite this version:

Julien Fontchastagner, Thierry Lubin, Smail Mezani, Noureddine Takorabet. Design optimization of an axial-field eddy-current magnetic coupling based on magneto-thermal analytical model. Open Physics, 2018, 16 (1), pp.21 - 26. 10.1515/phys-2018-0004 . hal-01728164

HAL Id: hal-01728164

<https://hal.science/hal-01728164>

Submitted on 10 Mar 2018

HAL is a multi-disciplinary open access archive for the deposit and dissemination of scientific research documents, whether they are published or not. The documents may come from teaching and research institutions in France or abroad, or from public or private research centers.

L'archive ouverte pluridisciplinaire **HAL**, est destinée au dépôt et à la diffusion de documents scientifiques de niveau recherche, publiés ou non, émanant des établissements d'enseignement et de recherche français ou étrangers, des laboratoires publics ou privés.

Research Article

Open Access

Julien Fontchastagner, Thierry Lubin*, Smaïl Mezani, and Noureddine Takorabet

Design optimization of an axial-field eddy-current magnetic coupling based on magneto-thermal analytical model

<https://doi.org/10.1515/phys-2018-0004>

Received October 31, 2017; accepted November 30, 2017

Abstract: This paper presents a design optimization of an axial-flux eddy-current magnetic coupling. The design procedure is based on a torque formula derived from a 3D analytical model and a population algorithm method. The main objective of this paper is to determine the best design in terms of magnets volume in order to transmit a torque between two movers, while ensuring a low slip speed and a good efficiency. The torque formula is very accurate and computationally efficient, and is valid for any slip speed values. Nevertheless, in order to solve more realistic problems, and then, take into account the thermal effects on the torque value, a thermal model based on convection heat transfer coefficients is also established and used in the design optimization procedure. Results show the effectiveness of the proposed methodology.

Keywords: Eddy-current, magnetic coupling, analytic thermal and magnetic model, optimal design

PACS: 41.20.Gz, 44.05.+e, 82.47.-a, 84.50.+d, 85.70.Ay

1 Introduction

An axial-flux eddy-current magnetic coupling consists of two discs facing each other (Figure 1). The driving disc is equipped with axially magnetized rare-earth permanent magnets regularly distributed to obtain alternately north and south poles. The driven disc is made up with a copper plate screwed to the back-iron [1–3]. The transmitted

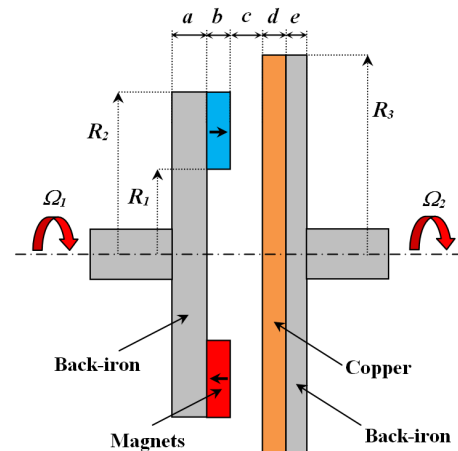


Figure 1: Axial-field eddy-current magnetic coupling with its geometrical parameters

torque of such a device is due to the interaction of magnets field and induced currents in the conducting plate which depend on the slip speed between the two discs. From its working principle, eddy-current coupling presents Joule losses, which are directly related to the slip speed. The normal working range area of such a device corresponds to low slip values for which the Joule losses are limited. The efficiency is given by $\eta = 1 - s$ where s is the slip ($s = (\Omega_1 - \Omega_2)/\Omega_1$).

The geometrical parameters of the studied coupler are given in Figure 1: R_1 is the inner radius of the magnets, R_2 the outer radius of the magnets, R_3 the outer radius of the copper plate, a is the thickness of the back-iron (magnets side), b the magnets thickness, c the air-gap length, d the thickness of the copper plate, e the thickness of the back-iron (copper side). The pole-arc to pole-pitch ratio of magnets is α , and p is the pole-pairs number. The mean radius of the torque coupler is defined as $R_m = (R_1 + R_2)/2$. The main objective of this paper is to determine the best design with reduced magnets volume and good efficiency.

For an accurate design of the eddy-current magnetic coupling, it is necessary to take into account the effects of the temperature on the copper conductivity. Due to the

Julien Fontchastagner: Université de Lorraine, GREEN, France, E-mail: julien.fontchastagner@univ-lorraine.fr

***Corresponding Author: Thierry Lubin:** Université de Lorraine, GREEN, France, E-mail: thierry.lubin@univ-lorraine.fr

Smaïl Mezani: Université de Lorraine, GREEN, France, E-mail: smail.mezani@univ-lorraine.fr

Noureddine Takorabet: Université de Lorraine, GREEN, France, E-mail: noureddine.takorabet@univ-lorraine.fr

eddy-current losses (heat source), the temperature of the copper will rise, so the electrical conductivity of the copper decreases. Hence, the produced torque decreases.

Very few papers discuss the thermal behavior of eddy-current magnetic couplings and its influence on their design, whereas it is a very important issue. Coupled magneto-thermal models, that can be found in the literature, are usually based on 2D or 3D finite elements (FE) simulations, considering either strong or weak coupling between the magnetic and thermal models [5–7]. Finite elements models give accurate results considering geometric details and nonlinearity for the materials behavior. However, they are still CPU time consuming and therefore poorly suited to be used in a design optimization procedure. In order to reduce the computational time, magnetic equivalent circuit (MEC) modeling coupled with thermal networks model have recently been developed [8, 9]. It has been shown that this method gives accurate results compared to FE simulations and tests. The main drawback of the MEC method is that the flux paths must be a priori known in order to define the reluctance expressions which appear in the torque expression [9].

In this paper, a complete design of an eddy-current magnetic coupling based on an electromagnetic-thermal coupled method is proposed. The optimization procedure is based on analytical formulas for the torque and the copper temperature. It is shown that the proposed models give results close to those obtained from 3D finite element simulations.

2 Preliminary design case

2.1 Analytic magnetic model

A torque formula (1) has been obtained from a 3D analytical model under the mean radius assumption. The mathematical developments are given in [1]. This formula depends directly on the physical and geometrical parameters of the coupler:

$$T_e = \frac{1}{2} \mu_0 p^2 \tau R_3 \Re \left[\sum_{n=1}^N \sum_{k=1}^K j k \frac{M_{nk}^2}{\alpha_{nk}} \underline{\tau} \sinh(\alpha_{nk} b) \right] \quad (1)$$

with:

$$M_{nk} = \frac{16 B_r}{\pi^2 \mu_0 n k} \sin \left(k \alpha \frac{\pi}{2} \right) \sin \left(n \frac{\pi R_2 - R_1}{2 R_3} \right); \quad \tau = \frac{\pi}{p} R_m$$

and:

$$\underline{\tau} = \frac{-(\cosh(\alpha_{nk} c) \sinh(\gamma_{nk} d) + \frac{\alpha_{nk}}{\gamma_{nk}} \sinh(\alpha_{nk} c) \cosh(\gamma_{nk} d))}{\cosh(\alpha_{nk}(b+c)) \sinh(\gamma_{nk} d) + \frac{\alpha_{nk}}{\gamma_{nk}} \sinh(\alpha_{nk}(b+c)) \cosh(\gamma_{nk} d)}$$

$$\alpha_{nk} = \sqrt{\left(\frac{n\pi}{R_3} \right)^2 + \left(\frac{k\pi}{\tau} \right)^2}$$

$$\gamma_{nk} = \sqrt{\left(\frac{n\pi}{R_3} \right)^2 + \left(\frac{k\pi}{\tau} \right)^2 + j \sigma \mu_0 \Omega R_m \frac{k\pi}{\tau}}$$

where n and k are odd integers, \Re denotes the real part of a complex number, $j = \sqrt{-1}$, σ is the electrical conductivity of the copper, B_r the remanence of the permanent magnets, and Ω is the slip speed.

The thickness of the back-irons (a and e , see Figure 1) should be determined to avoid magnetic saturation. For simplicity, we consider that the mean value of the flux density in the yokes must be under the knee point of the B-H curve (i.e $B < B_s$ with $B_s = 1.5\text{T}$). From the analytical model [1], we derived simple expressions to determine a minimal value for a and e :

$$a \geq 4 \frac{B_r R_m}{B_s \pi p} \sin \left(\alpha \frac{\pi}{2} \right) \left(1 - \frac{\sinh \left(\frac{\pi}{\tau} (c+d) \right)}{\sinh \left(\frac{\pi}{\tau} (b+c+d) \right)} \right) \quad (2)$$

$$e \geq 4 \frac{B_r R_m}{B_s \pi p} \sin \left(\alpha \frac{\pi}{2} \right) \frac{\sinh \left(\frac{\pi}{\tau} b \right)}{\sinh \left(\frac{\pi}{\tau} (b+c+d) \right)} \quad (3)$$

It is worth noting that $e < a$. In the following, a and e equal their corresponding minimal value, but they could be chosen bigger if required by mechanical constraints for instance.

2.2 First optimal design

The analytic model described in the previous section can be easily associated with an optimization algorithm in order to efficiently solve design problems [4]. The following problem is considered:

$$(P_1) \begin{cases} \min_{\mathbf{x} \in D} V_m(\mathbf{x}) \\ \text{with: } \mathbf{x} = [R_1, w_m, b, d, \alpha, p] \\ \text{subject to: } T_e(\mathbf{x}) \geq 50 \text{ N}\cdot\text{m} \\ R_3(\mathbf{x}) \leq 15 \text{ cm,} \end{cases} \quad (4)$$

where V_m is the total volume of magnets, w_m their radial extrusion ($w_m = R_2 - R_1$), and R_3 is calculated in order to permit a return path of the induced currents by: $R_3 = R_2 + \frac{\tau}{2}$ [1]. The remanence of magnets B_r is equal to 1.25 T, and the conductivity of copper is $57 \text{ MS}\cdot\text{m}^{-1}$. The airgap c is fixed to 3 mm. The considered operating point corresponds to a slip speed equal to 75 rpm for a driven speed $\Omega_1 = 1500$ rpm. The load power then equals 7.5 kW transmitted with a 95 % efficiency.

Problem (P_1) is relatively small: 6 variables (5 real and 1 integer) and 2 inequalities. It is sufficient to test the validity of the proposed design process. It belongs to the Mixed Integer Non-Linear Program (MINLP) problems class.

Table 1: Best found solution $\tilde{\mathbf{x}}_1$ of problem (P_1)

Variable	Bounds	Unit	Minimum
R_1	[4, 13]	cm	9.10
w_m	[2, 10]	cm	4.15
b	[4, 40]	mm	4.33
d	[2, 20]	mm	4.21
α	[0.6, 0.9]	-	0.71
p	[[2, 10]]	-	10
Quantity		Unit	Value
V_m		cm ³	89.0
T_e		N·m	50.0
R_3		cm	15.0

Since the model is purely analytic, each evaluation is very fast (less than 1 millisecond). Then the use of a meta-heuristic method with a huge number of evaluations does not require much CPU time. We choose a Particle Swarm Optimization (PSO) algorithm because of its simplicity of implementation [10]. A modified version of classical PSO accounting for integer variables (called MIPSPO) is implemented using MATLAB[®] software. Bounds constraints are handled by projection, and non-linear constraints by a penalty function. Therefore the initial optimization problem is transformed in an equivalent problem without non-linear constraint as follows:

$$\min_{\mathbf{x} \in D} \left(V_m(\mathbf{x}) + \mu_p \left[\max(0; 50 - T_e(x)) + \max(0; R_3(x) - 15 \cdot 10^{-2}) \right] \right) \quad (5)$$

For the following runs, the penalty factor μ_p has been chosen equal to 100. The initial swarm is generated using a latin hypercube sampling.

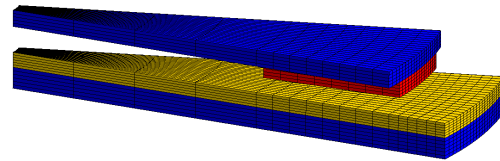
Since the used method cannot ensure with certainty the exactness of the solution, 10 different runs have been performed. A set of 200 particles evolving during 1000 iterations is used. Each run takes less than 30 seconds on a simple laptop (with Core i7 CPU @2.20 GHz). The best one $\tilde{\mathbf{x}}_1$ is given by Table 1.

3 Numerical validation and limitations of the previous methodology

3.1 Electromagnetic torque

In order to validate the solution obtained by the proposed design methodology, we have used a 3D finite element

model (FEM) to verify the torque value for $\tilde{\mathbf{x}}_1$. The authors have developed in [11] a complete 3D steady-state model, which takes into account the B-H curve of the iron yokes, and eddy currents in both copper and back iron. This model is developed using the free and open-source finite element solver GetDP [12]. The geometry and the corresponding mesh have been created with the free and open-source software Gmsh [13]. The yokes thicknesses a and e are calculated by (2) and (3): $a = 4.3$ mm and $e = 5.6$ mm. Figure 2 shows the geometry of one pole of $\tilde{\mathbf{x}}_1$ with its corresponding mesh.

**Figure 2:** Geometry and mesh of the optimal solution $\tilde{\mathbf{x}}_1$ (one pole)

With this FEM model, the calculated torque is 50.8 N·m, which proves the accuracy of the magnetic analytic model and demonstrates its relevance for an optimal design procedure as presented in the previous section.

3.2 Thermal aspects

In all of the described work, the temperature of the driven rotor and the corresponding thermal effects were neglected. The eddy current density is a heat source, which strongly influences the electrical conductivity of the copper σ . Figure 3 shows the variation of the copper conductivity as a function of the temperature θ :

$$\sigma(\theta) = \frac{\sigma_0}{1 + \alpha \theta} \quad (6)$$

where $\sigma_0 = 60 \text{ MS}\cdot\text{m}^{-1}$, and $\alpha = 3.93 \cdot 10^{-3} \text{ K}^{-1}$.

We propose here to simulate the designed coupling (corresponding to Table 1) thanks to a dedicated numerical formulation, which closely involves the magnetic field and the temperature (θ) resolution. In this global formulation, the heat equation is strongly coupled to a magnetic scalar potential (ϕ). Eddy current density is computed with a source field (\mathbf{h}_e), which exists in the copper and iron of the driven rotor. Only the steady-state operation is considered (see [11] for details on the used magnetic formulation). Both non-linearities, magnetic and thermal, are taken into account. The slip speed impacts both the eddy current density and the temperature distribution (by an advection term). The complete (\mathbf{h}_e , ϕ , θ) formulation is

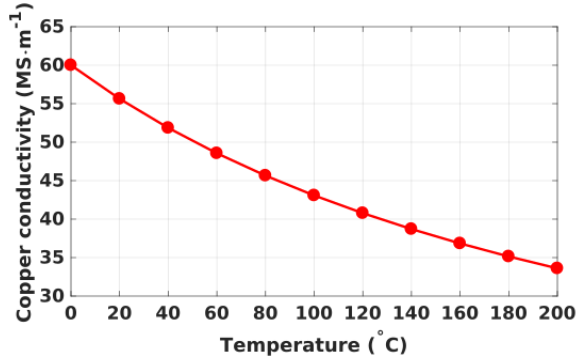


Figure 3: Copper conductivity as a function of the temperature

implemented in GetDP, and the resulting problem is solved using a fixed point method.

The obtained temperature distribution is plotted on Figure 4. At this point, the transmitted torque is only equal to 40.4 N·m (20% less than the expected value), due to the decrease of the copper electrical conductivity. These results clearly highlight that the temperature must be considered in the design problem, otherwise the optimal solution cannot fulfil the specifications.

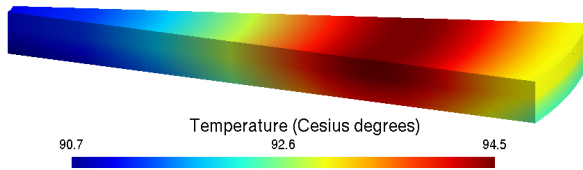


Figure 4: Temperature in the driven rotor for \tilde{x}_1 optimal solution (one pole)

4 Realistic design case

The copper disc of the studied eddy-current coupling is subjected to Joule losses, which depend on the slip speed. The generated heat leads to a diminution of the electrical conductivity of copper (Figure 3), which results in decreasing the produced torque. It is then necessary to consider the thermal aspects when sizing the coupling.

4.1 Analytic thermal model

Thermal analysis of eddy-current magnetic couplings has been performed by very few authors [3, 4], although this phenomenon has a great impact on the coupling perfor-

mances [14]. The thermal analysis is usually based on thermal network models, which give accurate results with less computational time than a purely numerical method i.e. finite element analysis. This is an important issue if the model has to be used in a design optimization procedure. Analytical models that can be found in the literature usually consider both heat conduction and heat convection in order to obtain the temperature distribution in each part of the magnetic coupling. Nevertheless, it was shown in [14], and confirmed by the results of Figure 4, that the temperature distribution in the copper and in the back-iron is almost homogeneous. This is particularly true when the magnetic coupling is used in the normal working range area, which corresponds to low slip values.

Then, a simple but realistic thermal model is considered in this paper. The following assumptions are adopted:

- Steady state conditions.
- The copper disc and back-iron thermal conductivities are high enough to neglect their thermal resistances.
- Only convection heat transfer through the external surfaces, whose convective heat transfer coefficients are noted h_1 and h_2 , is then considered.
- No heat exchange through the air-gap owing to its low film coefficient and air thermal conductivity [16].

In addition, this last assumption will give an excess value for the temperature in the copper, which goes in the right direction for the design.

The temperature of the copper θ is computed by:

$$\theta = \theta_a + \frac{P_J}{h_1 S_1 + h_2 S_2} \quad (7)$$

where $P_J = T_e \cdot s \Omega_1$ is the eddy current Joule losses, θ_a is the ambient temperature, which is fixed to 25°C, S_1 is the area of the cylinder surface normal to the radial direction, S_2 is the area of the cylinder surface normal to the axial direction:

$$S_1 = 2 \pi R_3 (d + e), \quad S_2 = \pi R_3^2 \quad (8)$$

In order to obtain a good prediction for the copper temperature, it is important to have a good estimation of the convective heat transfer coefficients h_1 and h_2 . The h_1 coefficient is usually determined by dimensionless analysis where the Nusselt number N_u has to be computed for the considered convection surface:

$$h_1 = \frac{k N_u}{2 R_3} \quad (9)$$

where k is the thermal conductivity of the fluid (air) at ambient temperature, and R_3 is the outer radius of the copper. For forced convection systems, the Nusselt number is usually given as a power law of the Reynolds number R_e and

Table 2: Thermal properties for air at ambient temperature (25°C)

Name	Description	Value	Unit
ρ	density	1.177	$\text{kg}\cdot\text{m}^{-3}$
k	thermal conductivity	0.0262	$\text{W}\cdot\text{m}^{-1}\cdot\text{K}^{-1}$
c_p	specific heat capacity	1006	$\text{J}\cdot\text{kg}^{-1}\cdot\text{K}^{-1}$
μ	dynamic viscosity	$1.84 \cdot 10^{-5}$	$\text{kg}\cdot\text{m}^{-1}\cdot\text{s}^{-1}$

the Prandtl number P_r :

$$N_u = a_1 R_e^{a_2} P_r^{a_3} \quad (10)$$

The values of the coefficients a_1 , a_2 , and a_3 depend on the fluid flow conditions. In our study, we have always set $R_e < 5 \cdot 10^5$ and then $a_1 = 0.084$, $a_2 = 0.70$, and $a_3 = 0.35$ (see [15] for details). The Reynolds and the Prandtl numbers that are used for calculating the Nusselt number are given by:

$$R_e = 2 \frac{\rho}{\mu} \Omega_2 R_3^2, \quad P_r = \frac{\mu c_p}{k} \quad (11)$$

The thermal properties of air are given in Table 2.

The coefficient h_2 can be determined by following the same method, but for a disk-type surface. In [15], a mean value for h_2 is given as:

$$h_2 = \frac{2 b_1}{2 b_2 + 1} \cdot \frac{k}{R_3} \left(\frac{\rho}{\mu} \Omega_2 R_3^2 \right)^{b_2} P_r^{b_3} \quad (12)$$

where $b_1 = 0.024$, $b_2 = 0.8$ and $b_3 = 0.6$.

From (9) to (12), we can note that the convective heat coefficients h_1 and h_2 depend on the coupling geometry and the rotating speed.

4.2 Optimal design accounting for temperature

The analytic thermal model described above is coupled to our analytic magnetic model thanks to the electrical conductivity of copper $\sigma(\theta)$. The resulting non-linear system is solved with a fixed point method, with a stopping criterion which corresponds to a relative difference between two successive temperature values less than 1%.

The initial optimal design (P_1) is amended in problem (P_2) to include thermal effects:

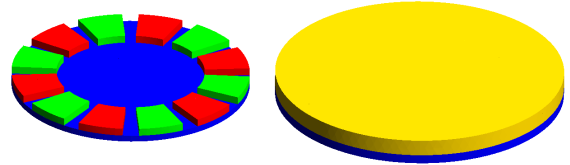
$$(P_2) \left\{ \begin{array}{l} \min_{\mathbf{x} \in D} V_m(\mathbf{x}) \\ \text{with: } \mathbf{x} = [R_1, w_m, b, d, \alpha, p] \\ \text{subject to: } T_e(\mathbf{x}, \theta(\mathbf{x})) \geq 50 \text{ N}\cdot\text{m} \\ R_3(\mathbf{x}) \leq 15 \text{ cm,} \\ \theta(\mathbf{x}) \leq 100 \text{ }^\circ\text{C} \end{array} \right. \quad (13)$$

Table 3: The best found solution $\tilde{\mathbf{x}}_2$ of problem (P_2) vs. $\tilde{\mathbf{x}}_1$ of (P_1): values computed with the magneto-thermal model

Variable	Bounds	Unit	$\tilde{\mathbf{x}}_1$ min (P_1)	$\tilde{\mathbf{x}}_2$ min (P_2)
R_1	[4, 13]	cm	9.10	7.71
w_m	[2, 10]	cm	4.15	4.67
b	[4, 40]	mm	4.33	8.05
d	[2, 20]	mm	4.21	17.1
α	[0.6, 0.9]	-	0.71	0.73
p	[[2, 10]]	-	10	6
Quantity			Values (with thermal effects)	
V_m		cm^3	89.0	173
T_e (analytic/numeric)		$\text{N}\cdot\text{m}$	40.0/40.4	50.0/50.8
θ average (ana./num.)		$^\circ\text{C}$	95.0/93.2	100/93.3
R_3		cm	15.0	15.0

The thermal phenomena are included both in the torque calculation and in a new constraint upon the average steady-state temperature in the copper disc. We impose a maximal value of 100°C in order to ensure an operating temperature of magnets under this limit value.

The same method of resolution used for problem (P_1) is applied. Each run of MIPS0 takes less than 80 seconds. The best found solution $\tilde{\mathbf{x}}_2$, after 10 runs, is given in Table 3 and compared to the previous one $\tilde{\mathbf{x}}_1$. The rotors (magnet side and copper side) for the geometry $\tilde{\mathbf{x}}_2$ are shown in Figure 5.

**Figure 5:** Geometry of the two rotors corresponding to $\tilde{\mathbf{x}}_2$

In accounting for the thermal effects, we can see that the solution obtained by problem (P_1) does not reach the specifications upon the torque (40 N·m instead of 50 N·m), as explained in Section 3.2. This is normal, since it has been sized with a fixed value for the electrical conductivity of copper (57 $\text{MS}\cdot\text{m}^{-1}$), whereas in reality it corresponds to the value at 95°C: $\sigma(\theta) \approx 43 \text{ MS}\cdot\text{m}^{-1}$. Then, there are less eddy currents and less torque. As a result, the temperature for $\tilde{\mathbf{x}}_1$ is slightly lower than for $\tilde{\mathbf{x}}_2$.

The new obtained solution $\tilde{\mathbf{x}}_2$ fulfills perfectly the specifications, which has been checked with the 3D FE numerical model ($T_e = 50.8 \text{ N}\cdot\text{m}$, $\theta = 93.3^\circ\text{C}$). It highlights the effectiveness of the developed coupled magnetic and

thermal analytic model, and clearly shows the relevance of the proposed methodology.

5 Conclusion

In this paper, an optimal design of an eddy-current magnetic coupling based on an analytic model is presented. The corresponding MINLP problem is solved thanks to a dedicated particle swarm optimization algorithm. If only the magnetic aspects are considered, the obtained optimal solution cannot fulfil the specifications. Then, a coupled magnetic and thermal model is proposed. It permits to solve a realistic optimal problem of design really efficiently, and this optimal solution has been verified by an numerical tool. Such a fast model is very accurate for any design process of eddy-current magnetic couplings.

References

- [1] Lubin T., Rezzoug A., 3-D analytical model for axial-flux eddy current couplings and brakes under steady-state conditions, *IEEE Trans. Magn.*, 2015, 51(10), 820371.
- [2] Davies E.J., An experimental and theoretical study of eddy-current couplings and brakes, *IEEE Trans. Power App. Syst.*, 1963, 82(67), 401-419.
- [3] Shin H.J., Choi J.Y., Cho H.W., Jang S.M., Analytical torque calculation and experimental testing of permanent magnet axial eddy current brake, *IEEE Trans. Magn.*, 2013, 49(7), 4152-4155.
- [4] Canova A., Vusini B., Design of axial eddy-current couplers, *IEEE Trans. Ind. Appl.*, 2003, 39(3), 1725-1733.
- [5] Gay S.E., Ehsani M., Parametric analysis of eddy-current brake performance by 3-D finite-element analysis, *IEEE Trans. Magn.*, 2006, 42(2), 319-329.
- [6] Zhang K., Li D., Zheng R., Yin W., Design and performance of a self-excited and liquid-cooled electromagnetic retarder, *IEEE Trans. Veh. Technol.*, 2015, 64(1), 13-20.
- [7] Ye L., Li D., Ma Y., Jiao B., Design and performance of a water-cooled permanent magnet retarder for heavy vehicles, *IEEE Trans. Energy Convers.*, 2011, 26(3), 953-958.
- [8] Gulec M., Yolacan E., Aydin M., Design analysis and real time dynamic torque control of single-rotor–single-stator axial flux eddy current brake, *IET Electr. Power Appl.*, 2016, 16(10), 869-876.
- [9] Mohammadi S., Mirsalim M., Design optimization of double-sided permanent-magnet radial-flux eddy-current couplers, *Electr. Power Syst. Res.*, 2014, 108, 282-292.
- [10] Kennedy J., Eberhart R., Particle swarm optimization, *Proceedings of IEEE International Conference on Neural Networks*, vol. 4., Perth, WA, 1995, 1942-1948.
- [11] Fontchastagner J., Lubin T., Netter D., Axial-field Eddy-current coupling: a 3D test problem for numerical experiments, *Int J Numer Model Electronic Networks, Devices and Fields*, in press, DOI: 10.1002/jnm.2217
- [12] Geuzaine C., GetDP: a general finite-element solver for the de Rham complex, *Proc. Appl. Math. Mech.*, 2008, 7(1), 603-604.
- [13] Geuzaine C., Remacle J.F., Gmsh: a three-dimensional finite element mesh generator with built-in pre- and post-processing facilities, *Int. J. Numer. Meth. Engng*, 2009, 79(11), 1309-1331.
- [14] Zheng D., Wang D., Li S., Shi T., Li Z., Yu L., Eddy current loss calculation and thermal analysis of axial-flux permanent magnet couplers, *AIP Advances*, 2017, 7(2), 025117
- [15] Roye D., Modélisation thermique des machines électrique tournantes, application à la machine à induction, PhD Thesis, INPG, Grenoble, France, 1983.
- [16] Howey D.A., Childs P.R.N., Holmes A.S., Air-Gap Convection in Rotating Electrical Machines, *IEEE Trans. Ind. Elec.*, 2012, 59(3), 1367-1375.